A Review and Update on Papillary Immature Metaplasia of the Uterine Cervix

A Distinct Subset of Low-Grade Squamous Intraepithelial Lesion, Proposing a Possible Cell of Origin

Soon Auck Hong, MD, PhD; Su Hyun Yoo, MD; Jene Choi, PhD; Stanley J. Robboy, MD; Kyu-Rae Kim, MD, PhD

• ***Context.***—**Papillary immature metaplasia (PIM) is a known papillary cervical lesion associated with low-risk human papillomavirus (LR-HPV).**

Objective.—**To evaluate additional clinicopathologic features and the HPV genotypes of PIM and discuss the presumptive cell of origin.**

Design.—**A total of 26 PIM cases were evaluated by $p16^{INK4a}$, cytokeratin (CK) 7, and CK17 immunohistochemical stainings. Human papillomavirus genotyping was performed, by using HPV DNA Chip, HPV polymerase chain reaction (PCR), and real-time PCR.**

Results.—**Histologically, PIM forms either a papillary mass (n = 21 of 26, 81%) or a slightly elevated/flat plaque (n = 5, 19%). All cases contain variable amounts of mucinous epithelia within the lesions. Koilocytosis was identified in 15 of the 26 cases (58%). Sixteen cases (61%) were associated with LR-HPV (types 6, 11, or 42), but 3 cases (12%) with high-risk (HR) HPV (16, 16/18, and 33), 2 cases (8%) with mixed LR- and HR-HPV (6/16 and 11/58), while 2 cases (8%) were negative, but $p16^{INK4a}$ immunostaining showed nonblock positivity in all cases. Eight (31%) had high-grade squamous intraepithelial lesion (HSIL) in the adjacent mucosa, 4 (50%) of which showed direct continuity. Identical HPV subtypes were confirmed in separately microdissected cases from PIM and adjacent HSIL. Most lesions (n = 24, 92%) expressed CK17 (reserve cell marker) in a bottom-heavy pattern and CK7 (squamocolumnar junction [SCJ] marker) in a top-heavy pattern, while most cases of low-grade squamous intraepithelial lesion (LSIL) were negative for both markers.**

Conclusions.—**Our results suggest that PIM is a distinct subset of LSIL showing a productive HPV infection, but PIM involves the transformation zone and is proximal to SCJ, while LSIL is mostly from ectocervix or distal to the SCJ.**

(*Arch Pathol Lab Med.* 2018;142:973–981; doi: 10.5858/arpa.2017-0267-OA)

Papillary immature metaplasia (PIM) of the uterine cervix, also called immature condyloma, was firstly described in 1992 by Ward et al[1] as a distinct subset of the exophytic low-grade squamous intraepithelial lesion (LSIL) associated with human papillomavirus (HPV).[1–4] Papillary immature metaplasia, although uncommon, is even more rarely identified owing to pathologists' poor recognition of the disease. Histologically, it consists of slender filiform papillae lined by squamous cells exhibiting varying degrees of cellular atypia and some loss of polarity. Thus, the lesion is easily misdiagnosed as papillary squamous cell carcinoma, condylomatous carcinoma, verrucous carcinoma, papillary high-grade squamous intraepithelial lesion (HSIL), atypical immature metaplasia, and condyloma acuminatum.[1,2,5] As implicated by the disease's name, PIM is a benign lesion with an epithelium that resembles metaplastic squamous epithelium, but with an uncertain cell of origin. Nevertheless, histopathogenetic relationship between PIM and LSIL has not been clarified.

Papillary immature metaplasia is associated with low-risk HPV, including types 6 and 11.[1,2,6,7] While the molecular biomarkers and HPV detection methods have improved significantly in recent years, the basic knowledge of PIM, including its associated HPV subtypes and precancerous potential, has not been updated. The recently developed HPV DNA Chip and semiquantitative real-time multiplex polymerase chain reaction (PCR) methods are PCR-based sensitive assays designed to detect high- and low-risk HPV genotypes. Cytokeratin (CK) 17 is found in subcolumnar

Accepted for publication October 23, 2017.
Published as an Early Online Release April 13, 2018.

From the Department of Pathology, Soonchunhyang University, Cheonan Hospital, Cheonan, Republic of Korea (Dr Hong); the Pathology Laboratory Department of U2Bio Co. Ltd., Seoul, Korea, and Department of Hospital Pathology, Uijeongbu St. Mary's Hospital, College of Medicine, The Catholic University of Korea, Uijeongbu, Republic of Korea (Dr Yoo); the Department of Pathology, University of Ulsan College of Medicine, Asan Medical Center, Seoul, Korea (Drs Choi and Kim); and the Department of Pathology, Duke University Medical Center, Durham, North Carolina (Dr Robboy). Dr Yoo is currently at the Pathology Laboratory Department of U2Bio Co. Ltd., Seoul, Korea.

The authors have no relevant financial interest in the products or companies described in this article.

Corresponding author: Kyu-Rae Kim, MD, PhD, Department of Pathology, Asan Medical Center, University of Ulsan College of Medicine, 88, Olympic-ro 43-gil, Songpa-gu, Seoul, 05505, Korea (email: krkim@amc.seoul.kr).

reserve cells, and immature metaplastic squamous epithelium, but not in columnar endocervical cells and squamous epithelium. Thus, it serves as a marker for cervical reserve cells, which give rise to metaplasia.[8] CK7 is used as a squamocolumnar junction (SCJ) marker by reacting with embryonic/stem cells and the cuboidal surface cells in the SCJ.[9–11]

In this study, we show that PIM is also associated with high-grade HPV phenotypes as in cases of LSIL, present additional clinicopathologic features, and discuss the presumptive cell of origin by comparing the expression patterns of $p16^{INK4A}$, Ki-67, CK17, and CK7 in 26 PIM cases with those of normal cervical mucosa and classic LSILs and HSILs.

MATERIALS AND METHODS

Case Selection

The institutional review board of Asan Medical Center (Seoul, Korea) approved this study (protocol 2014-1968-0001). Between 2000 and 2014, we collected 26 cases of papillary immature metaplasia or immature condyloma of the uterine cervix from the surgical pathology files at the Department of Pathology, University of Ulsan Collage of Medicine, Asan Medical Center. Histologic mimickers, including papillary HSIL, papillary squamous cell carcinoma, condyloma acuminatum, and reactive immature squamous metaplasia were carefully excluded by using previously described histopathologic findings and/or the immunoexpression patterns for $p16^{INK4A}$ and Ki-67. Papillary epithelial lesions demonstrating significant cytologic atypia and uniform block reactivity (positivity) for $p16^{INK4A}$ were excluded from the analyses.

The histopathologic features of 26 PIM cases were reviewed by 3 board-certified pathologists in a blinded fashion without additional clinical or cytologic information. The histopathologic analyses focused on the lesions' architecture at lower magnification, maturation status of the squamous epithelium, the presence or absence of mucin-secreting columnar epithelium, viral cytopathic effects (koilocytotic changes), and cellular atypia within the lesion. From the medical records, we obtained clinical information about age, chief complaints, cytologic diagnosis of the previous cervicovaginal smear at different institutions, clinical management, and follow-up.

Mucin Staining

Alcian blue (pH 2.5) and periodic acid–Schiff staining after diastase treatment (DPAS) were performed with a representative tissue section from each case according to standard protocols. The presence or absence of any scattered, clustered, or linearly aligned mucinous epithelia, within or on top of the papillary squamous epithelium, was recorded by using hematoxylin-eosin–, alcian blue–, and DPAS-stained sections.

Immunohistochemistry

To confirm the diagnosis and investigate the cell of origin, immunohistochemical staining for anti-$p16^{INK4A}$ (clone JC8, 1:200; Santa Cruz Biotechnology, Santa Cruz, California), Ki-67 (1:200; DAKO, Glostrup, Denmark), anti-CK17 (clone E3, 1:50; Novocastra, Newcastle, United Kingdom), and anti-CK7 (clone RCK 105, 1:1000; Abcam, Cambridge, United Kingdom) was conducted by using formalin-fixed, paraffin-embedded tissue sections and a Benchmark XT autoimmunostainer (Ventana Medical Systems, Tucson, Arizona) with the OptiView DAB detection kit (Roche Diagnostics, Mannheim, Germany). Briefly, 4-μm-thick sections were transferred onto silanized charged slides and dried for 10 minutes at room temperature, followed by 20 minutes in an incubator at 65°C. After standard heat-mediated epitope retrieval for 30 minutes in ethylenediaminetetraacetic acid (pH 8.0) in the autostainer, the samples were incubated with the primary antibodies to $p16^{INK4A}$, Ki-67, CK17, and CK7. The sections were subsequently incubated with biotinylated anti-mouse immunoglobulins, peroxidase-labeled streptavidin (LSAB kit; DAKO), and 3,3′-diaminobenzidine. Tissues containing cervical squamous cell carcinoma, normal tonsilar tissue, and normal breast tissue (for CK17 and CK7) were used as positive controls for $p16^{INK4A}$, Ki-67, CK17, and CK7, respectively; the negative control samples omitted the primary antibodies.

$p16^{INK4A}$ expression was assessed as nonreactive (negative, ie, no expression at all), nonblock positive, or block positive. Combined nuclear and cytoplasmic staining was interpreted as positive, but cytoplasmic staining only was interpreted as negative. The sample was considered "block positive" if it showed continuous strong nuclear or nuclear plus cytoplasmic staining of the basal cell layer with extension upward involving at least the lower third of the epithelial thickness,[12] whereas patch stainings or focally scattered reactivity in a few cells was interpreted as "nonblock positive." The Ki-67 labeling index was scored as the percentage of positive nuclei among 400 proliferating epithelial cells in hot spots. CK7 and CK17 were assessed as nonreactive, top-heavy, bottom-heavy, or diffuse patterns according to the presence or absence of an expression gradient across the cellular layers of the squamous epithelium. Seventeen cases of classic LSIL and 14 HSILs, the normal squamous and columnar epithelia in the mucosa adjacent to PIM, and the atrophic squamous epithelia from 10 postmenopausal women were included for comparison of immunoexpression patterns.

HPV Genotyping

Human papillomavirus genotyping was performed on all 26 cases by using 3 different methods: the HPV DNA Chip (GoodGene Co, Seoul, Korea) was used in 24 cases (92%), HPV polymerase chain reaction–restriction fragment length polymorphism (HPV PCR-RFLP) in 10 cases (38%), and semiquantitative real-time multiplex PCR (Anyplex II HPV28 Detection [Seegene, Seoul, Korea]) in 12 cases (46%). The latter 2 methods were used to confirm the negative results obtained by the HPV DNA Chip.

HPV DNA Chip

Detection using the HPV DNA Chip was performed in accordance with the manufacturer's protocols. Briefly, PCR amplification was performed by using 5 μg of DNA per reaction on a C1000 Thermal Cycler (Bio-Rad Laboratories Inc, Hercules, California) and a primer set targeting the *L1* gene of the HPV genome. β-Globin PCR amplification was performed as the internal control. The thermal cycling conditions consisted of an initial denaturation step at 95°C for 5 minutes, then 40 cycles at 95°C for 30 seconds, 50°C for 30 seconds, and 72°C for 30 seconds, followed by a final extension step at 72°C for 5 minutes. The PCR products were subjected to electrophoresis on a 2% agarose gel. The HPV and β-globin PCR products were 185 bp and 110 bp, respectively. For genotyping, 10 μL of each amplified product was denatured for 3 minutes at 95°C, mixed with the provided hybridization solution, and then spotted onto the DNA chip. The chip was subjected to a hybridization reaction at 48°C for 30 minutes in a hybridization chamber (Vision Scientific, Seoul, Korea). The chip was washed twice and dried at room temperature. The hybridized HPV DNA was identified by using a GoodGene DNA Chip Scanner (GoodGene Co, Seoul, Korea).

For the HPV DNA Chip, a PCR-based DNA microarray system was designed to detect 40 subtypes of HPV, including 21 high-risk (HPV-16, 18, 26, 31, 33, 35, 39, 45, 51, 52, 53, 56, 58, 59, 66, 67, 68a, 68b, 69, 70, and 73) and 19 low-risk (HPV-6, 11, 30, 32, 34, 40, 42, 43, 44, 54, 55, 61, 62, 72, 81, 83, 84, 90, and 91) types. Cases in which the DNA bound to universal probes, but without the signals for high- or low-risk HPV types, were interpreted as "unclassified" HPV types.

In 2 of the 8 samples in which PIM and HSILs were present in the same patients, microdissection was performed from paraffin-embedded section to separately collect tissues from each area of the PIM and HSIL by using the laser microdissection system (Leica LMD6500 Laser Microdissection System, Leica, Wetzlar, Ger-

many), as previously described.[13] Microdissected samples were lysed with QuickExtract DNA Extraction Solution (Epicentre, Madison, Wisconsin) for PCR analysis and separately genotyped. In the remaining 22 samples, DNA was extracted by using three 20-μm-thick sections of PIM lesions from archival blocks, but a special effort was made to exclude any surrounding nonlesional tissue.

HPV PCR: Restriction Fragment Length Polymorphism

We extracted HPV DNA from formalin-fixed paraffin blocks by using the QIAamp DSP DNA mini kit (Qiagen, Hilden, Germany). To detect low-risk HPV (types 6 and 11), the paired pU-1M/pU-2R primer was used, while the paired pU-31B/pU-2R primer was used to identify high-risk HPV (types 16, 18, 31, 33, 35, 52b, and 58). The primer sequences were as follows: pU-1M, 5′-TGTCAAAAACCGTGTGTCC-3′; pU-2R, 5′-GAGCTGTCGCTTAATTGCTC-3′; and pU-31B, 5′-TGCTAATTCGGTGCTACCTG-3′. The 25-μL reaction mixture contained 3 μL DNA (0.3 μg/μL), 2.5 μL buffer, 2 μL dNTP (200 μM dATP, dGTP, dCTP, and dTTP), 2 μL primer, 0.1 μL Taq (0.5 U), and 15.4 μL distilled water. Polymerase chain reaction amplification was performed with the C1000 Thermal Cycler (Bio-Rad Laboratories). Each cycle included a denaturation step at 94°C for 30 seconds, an annealing step at 55°C for 2 minutes, and a chain elongation step at 72°C for 2 minutes. The PCR product was electrophoresed on an agarose gel.

Semiquantitative Real-Time Multiplex PCR for HPV Genotyping Using Anyplex II HPV28 Detection

Semiquantitative real-time multiplex PCR for HPV genotyping was performed for 12 cases, which included 10 cases that demonstrated HPV-negative results on the HPV DNA Chip analysis. Genotyping was performed according to the manufacturer's instructions by using AnyplexTM II HPV28 Detection (Seegene) and a CFX96 real-time thermocycler (Bio-Rad Laboratories). HPV28 detection was designed to detect 20 high-risk HPV types (16, 18, 26, 31, 33, 35, 39, 45, 51, 52, 53, 54, 56, 58, 59, 66, 68, 69, 73, and 82) and 9 low-risk HPV types (6, 11, 40, 42, 43, 44, 54, 61, and 70). Briefly, PCR was implemented in a 20-μL volume, which consisted of 5 μL extracted DNA, 1× HPV28 TOM, and AnyplexTM PCR Mix (Seegene). An initial incubation at 50°C for 4 minutes, denaturation at 95°C for 15 minutes, and 50 cycles of denaturation (30 seconds at 95°C), annealing (1 minute at 60°C), and elongation (30 seconds at 72°C) were applied. Cyclic-catcher melting temperature analysis (CMTA) was used after 30, 40, and 50 PCR cycles. CMTA was performed by cooling the reaction mixture to 55°C, maintaining at 55°C for 30 seconds, and heating from 55°C to 85°. The HPV *L1* gene was amplified, and the internal control was human β-globin.

Statistical Analysis

The expression patterns of CK17 and CK7 in PIM, LSILs, and HSILs were compared by using the Fisher exact and χ^2 tests, and differences in the Ki-67 proliferation rate between PIM and HSILs were assessed by using the Mann-Whitney *U* test. In this study, $P < .05$ was considered statistically significant.

RESULTS

Clinical Findings

Clinically, all of the study patients were premenopausal, nonpregnant, healthy women of ages 24 to 52 years (median, 33.5 years). Lesions were incidentally discovered during the clinical workup for abnormal cervicovaginal smears in 22 of 26 patients (85%), and the remaining 4 patients (15%) presented with vaginal spotting, lower abdominal pain, endocervical polypoid mass, or leiomyoma, respectively. At different institutions, the cervicovaginal smears were diagnosed as atypical squamous cells of unknown clinical significance in 13 patients (50%), atypical squamous cells that cannot exclude high-grade squamous intraepithelial lesion in 2 patients (8%), HSIL in 2 patients (8%), LSIL in 5 patients (19%), atypical glandular cells of unknown significance in 1 patient (4%), reactive cellular change in 1 patient (4%), and negative in 2 patients (8%). Papillary or exophytic masses were observed by colposcopy in 9 patients (35%) or acetowhite in 10 patients (38%), but in 7 patients (27%) abnormal colposcopic findings were not described in their medical records. The masses were removed by loop electroexcision procedure (LEEP) in all but 1 patient, and the last patient underwent multiple punch biopsy. The margins of LEEP conization were clear in all 25 cases.

All patients were clinically followed up with cervicovaginal smears (range, 1–114 months; mean, 32.5 months), but abnormal cytologic features or recurrent masses were not again found.

Histopathologic Findings and Intracytoplasmic Mucin

At lower magnification, PIM formed an exophytic mass with thin fibrovascular cores in 21 of the 26 cases (81%; Figure 1, A), but in 5 cases (19%) it formed a slightly elevated, mildly undulated, or flat-topped plaque (Figure 1, B; Table 1). Exophytic masses consisted of filiform papillae reminiscent of condyloma acuminatum, but mostly lined by thick, proliferating, immature and mature squamous epithelial cells (Figure 1, C). In the flat-topped lesions, the squamous epithelium was markedly thickened by inverted growth mostly of basaloid cells, which formed anastomosing rete pegs extending into the underlying cervical stroma. Consequently, from the most basal to the most superficial layer, polarity of the epithelium was generally decreased both in exophytic and flat-topped lesions (Figure 1, C). All specimens disclosed varying degrees of mucin-secreting cells (Figure 1, D and E). In both papillary and flat-topped lesions, they formed numerous glands within the squamous epithelium. Mucin-secreting cells were aligned in a single continuous layer on the uppermost layers of the papillary fronds (Figure 1, D; and arrows), or frequently formed glandular structures (Figure 1, A and F; and arrows), or were individually scattered within the squamous epithelium (Figure 1, E; and arrows), and were easily demonstrated with alcian blue (pH 2.5) or DPAS.

Viral cytopathic (koilocytotic) changes were seen in 15 of the 26 cases (58%) and largely confined to the most mature squamous epithelium (Figure 1, E and F); they were absent in both the basaloid and immature squamous epithelium. The basaloid cells disclosed minimal cytologic atypia (Figure 1, C), whereas the "mature" squamous epithelium showed moderate nuclear hyperchromasia, irregular nuclear membranes, and occasional binucleation (Figure 1, E). The degree of cytologic atypia, however, was obviously less than that in HSIL or squamous cell carcinoma.

Eight of 26 cases (31%) were associated with flat HSIL in the adjacent mucosa, 4 (50%) of which demonstrated direct continuity between PIM and flat HSIL (Figure 2, A), but the remaining 4 cases (50%) had HSIL in the nearby mucosa in the same specimen, although not directly continuous. The PIM and flat HSIL were clearly distinguishable from each other by the differing degrees of cytologic atypia (Figure 2, A), Ki-67 labeling indices (Figure 2, B), and p16 immunoreactivity patterns (Figure 2, C).

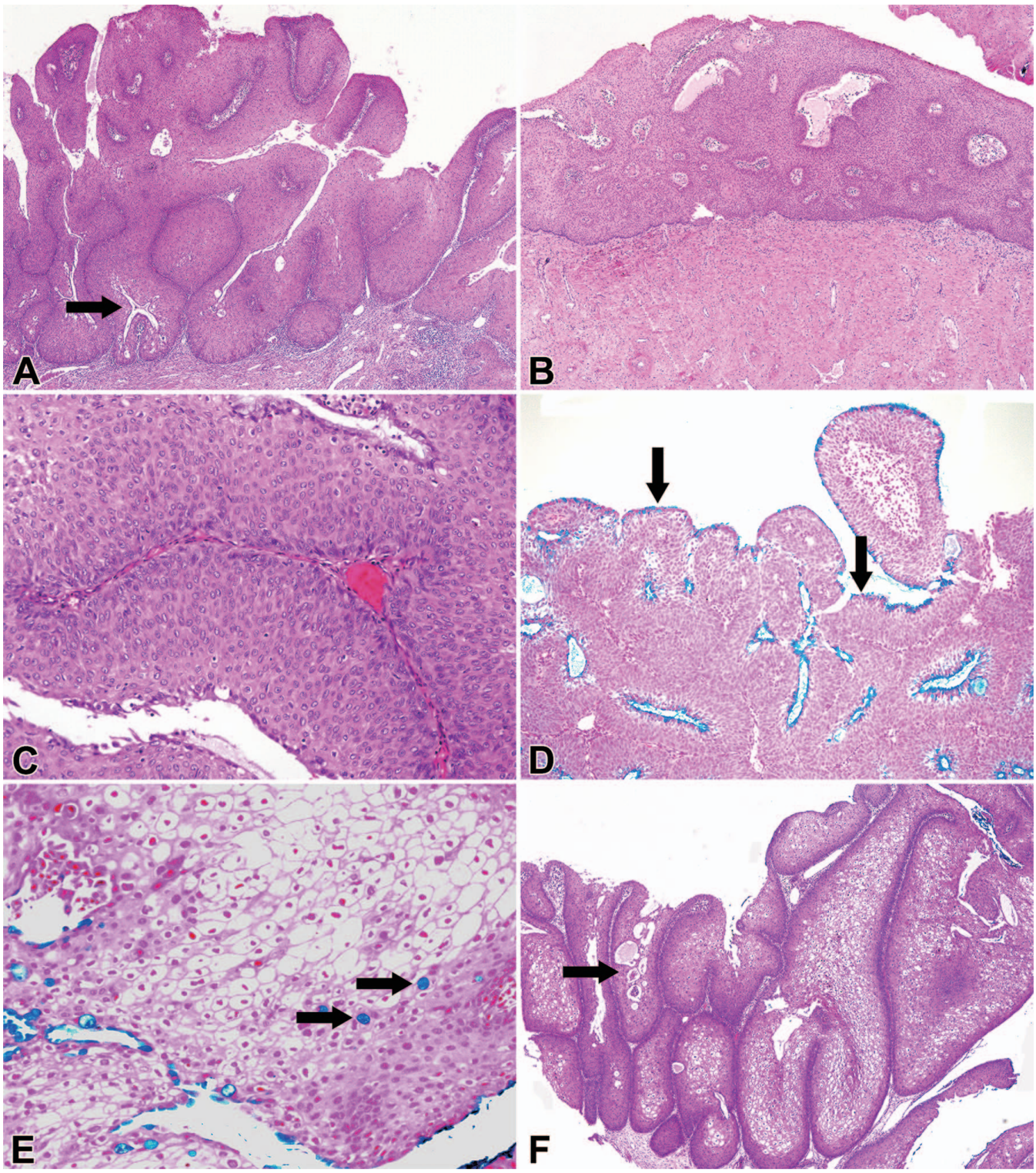

Figure 1. *Papillary immature metaplasia forming either an exophytic mass of filiform papillae (A) or a flat-topped lesion with the predominantly inverted growth of rete pegs (B). The lesional epithelium consists of a thick layer of proliferating basaloid and immature metaplastic cells (C), a variable proportion of which are mature. The mucinous epithelium is demonstrable, and linearly aligned atop the immature or mature squamous epithelium by alcian blue (D and E, arrows). Sometimes it forms glandular structures within the squamous epithelium (A and F, arrows) or is individually scattered within the nested squamous cells (E, arrows). Koilocytes are found exclusively in the mature squamous cells (E and F) (hematoxylin-eosin, original magnifications ×40 [A, B, and F] and ×200 [C]; alcian blue, original magnifications ×100 [D] and ×200 [E]).*

Table 1. Histopathologic Characteristics and Human Papillomavirus (HPV) Genotyping Results[a]

Case No.	Growth Pattern	Koilocytosis	Associated SIL	HPV (DNA Chip)	HPV PCR	HPV (Real-Time PCR)
1	Exophytic	+	HSIL	16	ND	ND
2	Exophytic	−	HSIL	16, 18	ND	ND
3	Flat	−	−	Neg	Neg	42
4	Exophytic	+	−	11	ND	ND
5	Exophytic	+	−	HPV, unclassified	ND	ND
6	Flat	−	HSIL	Neg	Neg	Not amplified
7	Exophytic	−	−	Neg	Neg	Neg
8	Exophytic	+	−	Neg	Neg	Not amplified
9	Exophytic	+	−	11	ND	ND
10	Flat	+	−	Neg	Neg	6
11	Exophytic	−	−	11	ND	ND
12	Exophytic	+	−	11	ND	ND
13	Exophytic	+	−	6	ND	ND
14	Exophytic	+	−	11	ND	ND
15	Flat	−	HSIL	11	ND	ND
16	Exophytic	+	−	Neg	LR-HPV	6
17	Exophytic	−	−	11	ND	ND
18	Exophytic	−	−	6	ND	ND
19	Exophytic	−	−	6	ND	ND
20	Exophytic	−	HSIL	Neg	Neg	33
21	Exophytic	−	−	Neg	Neg	Neg
22	Exophytic	+	HSIL	Neg	LR-HPV	6
23	Exophytic	+	−	Neg	LR-HPV	6
24	Exophytic	+	−	11	ND	ND
25	Flat	+	HSIL	ND	ND	6, 16
26	Exophytic	+	HSIL	ND	ND	11, 58

Abbreviations: HSIL, high-grade squamous intraepithelial lesion; LR-HPV, low-risk human papillomavirus types; ND, not done; Neg, negative; PCR, polymerase chain reaction; SIL, squamous intraepithelial lesion; +, present; −, absent.

[a] All cases disclosed nonblock positivity for $p16^{INK4a}$.

Immunohistochemical Expression

The Ki-67 labeling index of PIM ranged from 10% to 56% (mean, 24%), which exceeded that of the normal squamous epithelium, but was significantly lower than that of HSIL (range, 64%–92%; mean, 79%; $P < .001$). The Ki-67 immunostaining showed basal/parabasal positivity with upward extension in 24 cases (Figure 2, B; and open arrow), but in 2 of 5 cases forming a flat-topped plaque, Ki-67 labeling index was significantly decreased in basal/parabasal layers as well as in the upper epithelium. Papillary lesion with prominent koilocytosis showed significantly increased Ki-67 positivity in the upper epithelium in addition to the basal/parabasal positivity (Figure 2, B; and open arrow); in contrast, the Ki-67–labeled cells were confined to the parabasal and/or basal cell layers in normal or atrophic squamous epithelia. The difference in the Ki-67 labeling index between PIM and HSILs was well demonstrated in the same specimen (Figure 2, B).

$p16^{INK4a}$ staining showed patchy, nonblock positivity in all PIM cases with various intensities (Figure 2, C; and open arrow), but the basal and parabasal layers were mostly spared. The HSILs in the adjacent mucosa (Figure 2, B; and closed arrow) and the 14 HSILs included as the control group demonstrated extensive and strong reactivity in the entire layers or in the basal and parabasal cells layers.

CK17 was normally expressed in the cytoplasm of the subcolumnar reserve cell layer and immature squamous metaplasia (Figure 3, A), but not in the apically located mucin-containing columnar epithelium and mature, or atrophic, squamous epithelia. In PIM, CK17 reactivity was exclusively found only in the basal layers in 10 of the 26 cases (38%) or in both the basal and parabasal layers in 14

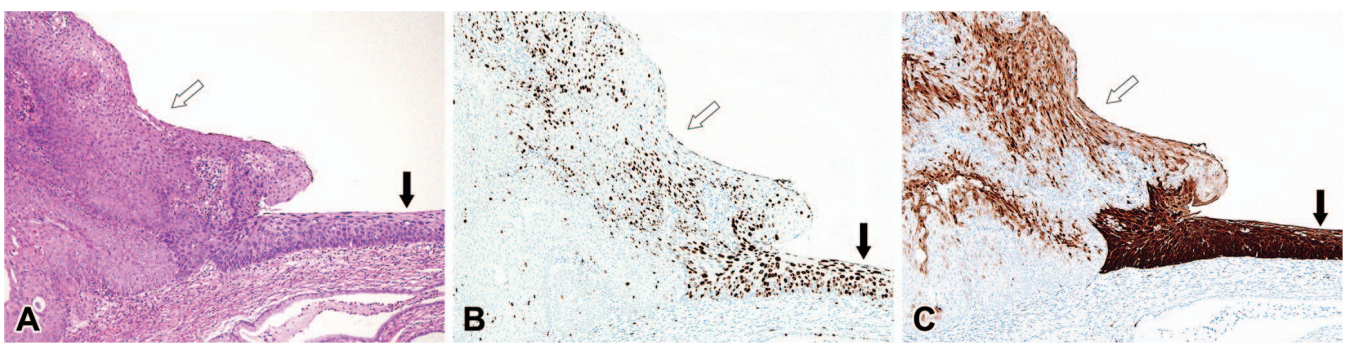

Figure 2. *A flat high-grade squamous intraepithelial lesion (HSIL) lies in direct continuity with the mucosa adjacent to the papillary immature metaplasia (PIM) (A); however, PIM (open arrow) and HSIL (closed arrow) are easily distinguishable owing to the different degrees of cytologic atypia (A), Ki-67 labeling index in PIM (open arrow) and HSIL (closed arrow) (B), and different $p16^{INK4}$ expression patterns in PIM (open arrow) and HSIL (closed arrow) (C) (hematoxylin-eosin, original magnification ×40 [A]; original magnification ×40 [B and C]).*

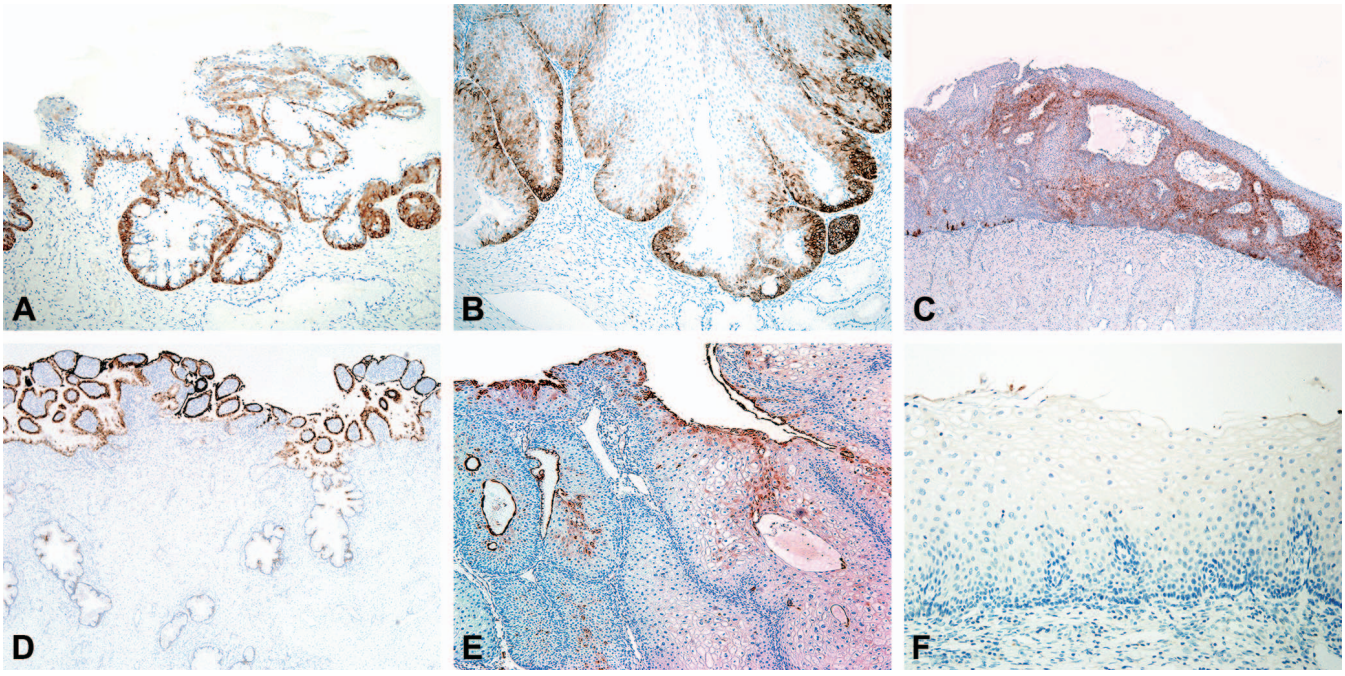

Figure 3. *Cytokeratin (CK) 17, a reserve cell marker, is exclusively expressed in the reserve cells and immature squamous metaplasia in the normal cervical mucosa (A). Papillary immature metaplasia (PIM) demonstrates a bottom-heavy pattern in most exophytic lesions (B), but flat-topped lesions that consisted largely of basaloid cells demonstrate diffuse expression throughout the entire squamous epithelia (C). CK7, a known squamocolumnar junction marker, appears in the columnar cells within the transformation zone and superficial portion of the glands, but not in the upper endocervix or deeper portions of the endocervical glands in the normal cervical mucosa (D). In papillary immature metaplasia, CK7 appears only in the overlying mucinous epithelium on top of the PIM or in a top-heavy pattern (E). Low-grade squamous intraepithelial lesion is completely negative for CK7 (F) (original magnifications ×40 [C and D]; ×100 [A, B, and E]; and ×200 [F]).*

cases (54%) (Figure 3, B), producing a prominently bottom-heavy pattern in 24 cases (92%). However, 2 cases (8%) exclusively composed of basaloid cells showed diffuse expression of CK17 throughout all layers (Figure 3, C). In contrast to PIM, the LSIL specimens usually showed no expression in 14 cases (82%), diffuse expression in 1 case (6%), and basal expression in the remaining 2 cases (12%). Fourteen HSIL cases demonstrated bottom-heavy patterns in 6 cases (43%), diffuse expression in 5 cases (36%), and complete negativity in 3 cases (21%).

In the normal cervix, CK7 was normally expressed in the superficial opening portion of the endocervical glands at the SCJ (Figure 3, D), but not in the proximal endocervix or deeper portions of the endocervical glands (Figure 3, D). In PIM, CK7 expression was identified either in the superficial columnar cells atop the papillary lesions only (18 cases; 69%) or in the columnar and superficial squamous epithelia (6 cases; 23%), producing a top-heavy pattern in 24 cases (92%) (Figure 3, E). Uniformly intense cytoplasmic immunoreactivity of the entire epithelium was not observed. In contrast, LSIL demonstrated complete nonreactivity (Figure 3, F) in all but 1 case (16 of 17 cases; 94%), indicative of a significantly different expression pattern from PIM (Table 2). HSIL showed either a top-heavy expression pattern (10 of 14 cases; 71%) or negativity (4 of 14 cases; 29%).

HPV Genotypes

Using the HPV DNA Chip method, 11 PIM specimens (11 of 24; 46%) disclosed low-risk HPV types (8 patients with HPV-11 [8 of 11; 73%], and 3 patients with HPV-6 [3 of 11; 27%]); 2 cases (2 of 24; 8%) with high-risk types (1 patient with HPV-16 and 1 patient with mixed HPV-16/18); 1 unclassified type (1 patient [4%]); and 10 cases (10 of 24; 42%) with no demonstrable HPV (Table 1).

Ten HPV-negative cases were regenotyped by using HPV PCR-RFLP. Three more cases (3 of 10; 30%) were associated with low-risk HPV types (6 or 11), and 7 cases (7 of 10; 70%) were negative (Table 1). Twelve cases (12 of 26; 46%), including 10 cases showing HPV-negative results according to the HPV DNA Chip test and an additional 2 cases that

Table 2. Expression of p16^{INK4a}, Cytokeratin (CK) 17, and CK7 in Papillary Immature Metaplasia, Low-Grade and High-Grade Squamous Intraepithelial Lesions[a]

	p16^{INK4a}	CK17				CK7		
	Nonblock Positivity	Bottom-Heavy Pattern	Diffuse	Negative	Top-Heavy Pattern	Negative	Diffuse	*P*
PIM, No. (%)	26 (100)	24 (92)	2 (8)	0 (0)	24 (92)	2 (8)	0 (0)	<.001
LSIL, No. (%)	ND	2 (12)	1 (6)	14 (82)	1 (6)	16 (94)	0 (0)	<.001
HSIL, No. (%)	ND	6 (43)	5 (36)	3 (21)	10 (71)	4 (29)	0 (0)	<.001

Abbreviations: HSIL, high-grade squamous intraepithelial lesion; LSIL, low-grade squamous intraepithelial lesion; ND, not done; PIM, papillary immature metaplasia.

[a] Expression of CK17 and CK7 in PIM, LSIL, and HSIL was evaluated by Fisher exact tests and χ^2 tests.

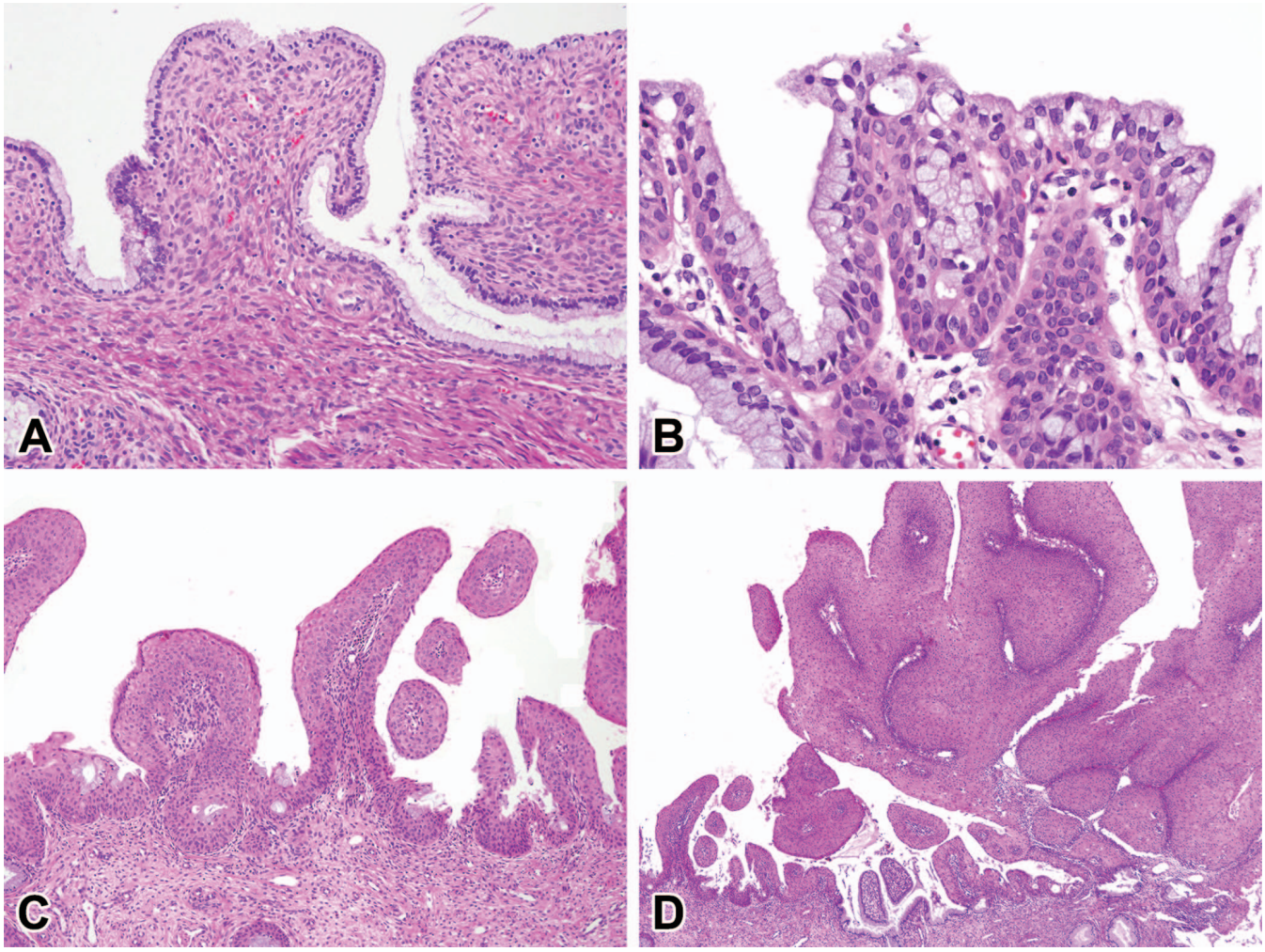

Figure 4. *The presumed pathogenetic mechanism of origin of papillary immature metaplasia. The normal endocervical mucosa forms either a flat or micropapillary configuration composed of single layer of columnar epithelium (A), from which the reserve cells are differentiated according to "top-down differentiation" (B). They further proliferate and differentiate to form the early stage of immature metaplasia by "upward proliferation and differentiation" (C) and progress to form papillary immature metaplasia (D) (hematoxylin-eosin, original magnifications ×200 [A], ×400 [B], ×100 [C], and ×40 [D]).*

were not available for DNA Chip test, were reexamined with semiquantitative real-time multiplex PCR. Additionally, HPV-42 (1 of 12; 8%), HPV-6 (4 of 12; 33%), HPV-33 (1 of 12; 8%), mixed HPV-6/16 (1 of 12; 8%), and HPV-11/58 (1 of 12; 8%) were detected, and 2 cases (2 of 12; 17%) were negative for HPV (Table 1). Two cases (2 of 12; 17%) were excluded owing to the low quality of the DNA content.

Collectively, 2 PIM cases (2 of 26; 8%) were negative on HPV genotyping using all 3 detection methods. Eighteen PIM cases (18 of 26; 69%), which were not accompanied by HSIL, were associated with HPV-6 (6 of 18; 33%), HPV-11 (7 of 18; 39%), HPV-42 (1 of 18; 6%), or an unclassified HPV type (1 of 18; 6%). However, 8 PIM cases (8 of 26; 31%) accompanied by HSIL in the adjacent mucosa were associated with purely high-risk HPV types in 3 cases (3 of 8; 37.5%) (HPV-16, HPV-16/18, and HPV-33), mixed high- and low-risk HPV in 2 cases (2 of 8; 25.0%) (HPV-6/16 and HPV-11/58), low-risk HPV in 2 cases (2 of 8; 25.0%) (HPV-6 and HPV-11), and HPV negativity in 1 case (1 of 8; 12.5%). The 2 cases in which the tissues were separately microdissected from both PIM and HSIL contained the same HPV types in both lesions (HPV-11/58 and HPV-6/16).

DISCUSSION

Papillary immature metaplasia is a lesion with a known association to low-risk HPV types, including types 6 and 11.[1,2,6,7,14] Although PIM and HSIL may coexist in the same patient,[7,14] its premalignant potential or progression to HSIL has rarely been discussed. In our current study, PIM was sometimes found to be associated with HSIL in the adjacent mucosa (8 of 26; 31%) as in cases of LSIL, half of which demonstrated direct continuity from PIM to HSIL (Figure 3, A). Five PIM cases (19%) were associated with either high-risk HPV only or mixed high- and low-risk HPV types (Table 1). The same HPV subtypes, HPV-11/58 and HPV-6/16, were detected in both PIM and HSIL in 2 cases, which were identified in separately microdissected specimens. These findings suggest that PIM potentially can progress to HSIL.

Recently, the target cell of HPV in cervical carcinogenesis has become a focus of interest.[9–11] Slow-cycling epithelial stem cells or progenitor cells at the SCJ, so-called SCJ cells,

have recently been proposed as the prime target cells for HPV in cervical carcinogenesis.[9–11,15] In this study, however, we postulated that both PIM and LSIL represent productive HPV infections adjacent to the SCJ and involving the transformation zone, but the 2 lesions are derived from different types of cells. Papillary immature metaplasia could be derived from a more proximal portion of the SCJ toward the endocervix, compared to LSIL, since PIM is frequently found in the more proximal portion of the cervix toward the endocervix clinically,[1] almost always contains mucin-secreting cells, and generally expresses CK7 and CK17, whereas LSILs are almost entirely composed of mature squamous epithelia, with polarity relatively well preserved, demonstrate prominent koilocytotic changes, rarely contain mucin-secreting epithelia, and rarely express CK7 or CK17. Recently, Herfs et al[9] segregated LSIL into SCJ-marker-positive and SCJ-marker-negative subsets, using SCJ specific antibodies, and found that SCJ-marker-positive subset had a significantly higher incidence of $p16^{ink4}$ block positivity and HSIL outcomes in the follow-up. From the SCJ marker status, they proposed that SCJ-positive subset could be derived from "SCJ cells," while SCJ-negative subset came from ectocervix or distal part of the SCJ cells.[9] Most of the LSIL cases included in our study were SCJ negative (16 of 17; 94%) and had different CK7/17 expression patterns, indicating that most of the SCJ-negative LSILs could be derived from cells in ectocervix or distal to the SCJ cells, while PIM came from cells in endocervix or proximal to the SCJ cells.

Histologically, PIM has a significantly increased proportion of basaloid and immature squamous epithelia, resulting in partial or significant loss of polarity, while LSIL is predominantly composed of mature squamous epithelium. In previous studies of PIM, koilocytotic changes were rarely observed,[2] but in our study, we observed it in 15 patients (58%). Papillary immature metaplasia has relatively fewer koilocytes than LSILs, and the koilocytes were mostly confined to the smaller areas composed of mature squamous epithelium, but not in the areas of basaloid or immature squamous epithelia. Since the koilocyte is formed when the intermediate filaments in terminally differentiated squamous cells undergo destruction in order to release the virus,[16,17] the low incidence of koilocytosis might reflect the more immature status of the PIM compared to LSILs.

The frequently observed papillary architecture of PIM also supports the origin from the more proximal portion of the cervix. The normal endocervical mucosa proximal to the SCJ shows either a flat or micropapillary configuration (Figure 4, A). The flat or micropapillary endocervical mucosa consists of a stromal core covered with a single layer of the columnar epithelium. As the transformation zone remodels, the CK17-expressing reserve cell layer becomes prominent beneath the columnar epithelium by "top-down" differentiation, in which precursor cells are more apically located to the differentiated cells[10] (Figure 4, B). Then, as the reserve cells proliferate and differentiate toward the immature and mature squamous epithelium (Figure 4, C), the daughter cells continuously stack above the reserve cell layer beneath the apical columnar epithelium (Figure 4, D). The stepwise pathogenesis of PIM is summarized in Figure 5. The intensity of CK17 staining dilutes as the reserve cells differentiate upward, which forms the bottom-heavy pattern of CK17 immunostaining (Figure 3, B). Depending on the degree of maturation of the squamous epithelium, CK17 expression demonstrated either a bottom-heavy (Figure 3, B) or diffuse pattern (Figure 3, C) (Table 2). In our study, the extent of mature squamous differentiation, polarity of the squamous epithelium, and CK17 expression, either diffuse or bottom-heavy pattern, were well correlated. In cases where the PIM is mostly composed of basaloid cells, the lesion mimicked HSIL or papillary squamous cell carcinoma owing to significant loss of polarity. CK17 expression showed a diffuse expression pattern throughout entire layers (Figure 3, C), while in cases where the lesions are predominantly composed of immature or mature squamous epithelia, the polarity is relatively well preserved, koilocytotic changes are frequent, and CK17 expression demonstrates a bottom-heavy pattern (Figure 3, B).

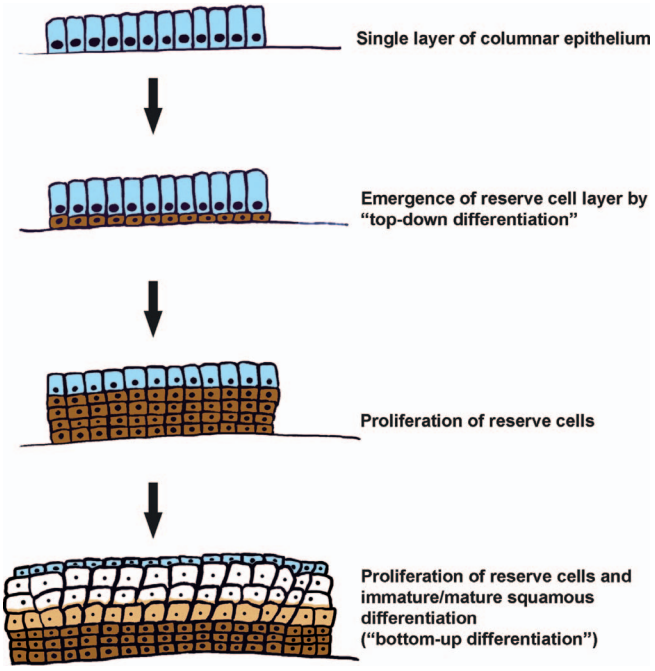

Figure 5. *The stepwise pathogenesis of papillary immature metaplasia.*

Papillary immature metaplasia typically discloses a characteristic filiform papillary growth, but 5 patient specimens (5 of 26; 19%) in our group showed only slightly elevated or flat-topped plaques with the predominantly inverted growth of squamous epithelium. Considering that PIM is possibly derived from the more proximal part of the transformation zone, where the normal mucosa has either a flat or micropapillary configuration, a flat-topped plaque and/or a predominantly inverted growth pattern should also be included as an additional PIM growth pattern.

Currently, the gold standard method for HPV detection has not been determined. Every method or combination of methods has specific drawbacks. In our current study, the genotyping agreement rate among the 3 detection methods could not be compared, since HPV PCR and real-time PCR methods were used as confirmative tests for the HPV-negative cases determined with HPV DNA Chip; however, HPV DNA Chip and HPV PCR demonstrated lower detection rates than real-time PCR (Table 1). In our study, every PIM case including the 2 HPV-negative cases by HPV genotyping methods showed nonblock $p16^{INK4}$ immunoreactivity. The HPV DNA–negative results could result from the genotyping method's low sensitivity or extremely low *L1* gene copy number.[18] However, Rietbergen et al[19] found that

integration of HPV DNA may result in the interruption of the viral genome in a region that may extend anywhere from the E1 to the L1 open reading frame in the p16-immunopositive/HPV DNA–negative cases. Considering that HPV genotyping methods target a sequence from the L1 region of HPV genome, integration-associated gross deletion and mutation of the viral genome in the L1 region may result in the p16-immunopositive but HPV DNA–negative cases.[19] Therefore, immunohistochemical staining for $p16^{INK4}$ seems to be a reliable surrogate marker for HPV detection.

In summary, our study indicates that PIM is a form of LSIL caused by productive HPV infection, and may have an association with high-risk–type HPV and progression to HSIL in some cases. The histopathologic features of either a flat or papillary configuration appear to depend on the prior mucosal pattern (flat or micropapillary), and basaloid versus squamoid cellular component is determined by the degree of maturation toward immature and mature squamous epithelia. However, it is not yet known which factors cause PIM in endocervical cells proximal to "SCJ cells" that will be vulnerable to HPV infection.

References

1. Ward B, Saleh A, Williams J, Zitz J, Crum C. Papillary immature metaplasia of the cervix: a distinct subset of exophytic cervical condyloma associated with HPV- 6/11 nucleic acids. *Mod Pathol*. 1992;5(4):391–395.
2. Mosher RE, Lee KR, Trivijitsilp P, Crum CP. Cytologic correlates of papillary immature metaplasia (immature condyloma) of the cervix. *Diagn Cytopathol*.1998;18(6):416–421.
3. Park J-J, Genest DR, Sun D, Crum CP. Atypical immature metaplastic-like proliferations of the cervix: diagnostic reproducibility and viral (HPV) correlates. *Hum Pathol*. 1999;30(10):1161–1165.
4. Liang C-W, Lin M-C, Hsiao C-H, Lin Y-T, Kuo K-T. Papillary squamous intraepithelial lesions of the uterine cervix: human papillomavirus-dependent changes in cell cycle expression and cytologic features. *Hum Pathol*. 2010;41(3): 326–335.
5. Crum CP, Egawa K, Fu YS, et al. Atypical immature metaplasia (AIM): a subset of human papilloma virus infection of the cervix. *Cancer*. 1983;51(12): 2214–2219.
6. Trivijitsilp P, Mosher R, Sheets EE, Sun D, Crum CP. Papillary immature metaplasia (immature condyloma) of the cervix: a clinicopathologic analysis and comparison with papillary squamous carcinoma. *Hum Pathol*. 1998;29(6):641–648.
7. Kang GH, Min K, Shim YH, Kim KR. Papillary immature metaplasia of the uterine cervix: a report of 5 cases with an emphasis on the differential diagnosis from reactive squamous metaplasia, high-grade squamous intraepithelial lesion and papillary squamous cell carcinoma. *J Korean Med Sci*. 2001;16(6):762–768.
8. Smedts F, Ramaekers FC, Vooijs PG. The dynamics of keratin expression in malignant transformation of cervical epithelium: a review. *Obstet Gynecol*. 1993; 82(3):465–474.
9. Herfs M, Herran CP, Howitt B, et al. Cervical squamocolumnar junction-specific markers define distinct, clinically relevant subsets of low-grade squamous intraepithelial lesions. *Am J Surg Pathol*. 2013;37(9):1311–1318.
10. Herfs M, Vargas SO, Yamamoto Y, et al. A novel blueprint for 'top down' differentiation defines the cervical squamocolumnar junction during development, reproductive life, and neoplasia. *J Pathol*. 2013;229(3):460–468.
11. Herfs M, Yamamoto Y, Laury A, et al. A discrete population of squamocolumnar junction cells implicated in the pathogenesis of cervical cancer. *Proc Natl Acad Sci U S A*. 2012;109(26):10516–10521.
12. Darragh TM, Colgan TJ, Cox JT, et al. The lower anogenital squamous terminology standardization project for HPV-associated lesions: background and consensus recommendations from the College of American Pathologists and the American Society for Colposcopy and Cervical Pathology. *Arch Pathol Lab Med*. 2012;136(10):1266–1297.
13. Eriksen AHM, Andersen RF, Pallisgaard N, Srensen FB, Jakobsen A, Hansen TF. MicroRNA expression profiling to identify and validate reference genes for the relative quantification of microRNA in rectal cancer. *PLoS One*. 2016;11(3): e0150593.
14. Roberts JM, Cornall AM, Ekman D, et al. Papillary immature metaplasia of the anal canal: a low-grade lesion that can mimic a high-grade lesion. *Am J Surg Pathol*. 2016;40(3):348–353.
15. Cid Arregui A, Gariglio P, Kanda T, Doorbar J. Oncogenic human papillomaviruses: high-risk human papillomaviruses: towards a better understanding of the mechanisms of viral transformation, latency and immune-escape. *Open Virol J*. 2011;6:160–162.
16. Doorbar J, Quint W, Banks L, et al. The biology and life-cycle of human papillomaviruses. *Vaccine*. 2012;30 (suppl 5):F55–F70.
17. Nguyen HP, Ramírez-Fort MK, Rady PL. The biology of human papillomaviruses. In: *Human Papillomavirus*. Vol 45. Basel, Switzerland: Karger Publishers; 2014:19–32.
18. Kwon M-J, Roh KH, Park H, Woo H-Y. Comparison of the Anyplex II HPV28 assay with the Hybrid Capture 2 assay for the detection of HPV infection. *J Clin Virol*. 2014;59(4):246–249.
19. Rietbergen MM, Snijders PJ, Beekzada D, et al. Molecular characterization of p16-immunopositive but HPV DNA-negative oropharyngeal carcinomas. *Int J Cancer*. 2014;134(10):2366–2372.